

Imaging of Myocardial Ischemia–Reperfusion Injury Using Sodium [^{18}F]Fluoride Positron Emission Tomography/Computed Tomography in Rats and Humans

Hongyoon Choi, MD, PhD¹, Jeong Hee Han, PhD¹, Sue Yeon Lim, MS¹, Inki Lee, MD¹, Young-Seok Cho, MD, PhD², Eun Ju Chun, MD, PhD³, and Won Woo Lee, MD, PhD^{1,4}

Abstract

Positron emission tomography (PET)/computed tomography (CT) using sodium [^{18}F]fluoride ($\text{Na}[^{18}\text{F}]\text{F}$) has been proven to be a promising hot-spot imaging modality for myocardial infarction (MI). We investigated $\text{Na}[^{18}\text{F}]\text{F}$ uptake in ischemia–reperfusion injury (IRI) of rats and humans. Sodium [^{18}F]fluoride PET/CT was performed in Sprague-Dawley rats that had IRI surgery, and it readily demonstrated prominent $\text{Na}[^{18}\text{F}]\text{F}$ uptake in the infarct area post-IRI. Sodium [^{18}F]fluoride uptake was matched with negative 2,3,5-triphenyl-2H-tetrazolium chloride staining results, accompanied by myocardial apoptosis and associated with positive calcium staining results. Furthermore, area at risk was negative for $\text{Na}[^{18}\text{F}]\text{F}$ uptake. Cyclosporine A (CysA) treatment reduced standardized uptake value of ^{18}F over the infarct area, and a significant decrease in infarct size was also observed by the CysA treatment. In humans, $\text{Na}[^{18}\text{F}]\text{F}$ PET/CT readily demonstrated increased $\text{Na}[^{18}\text{F}]\text{F}$ uptake in the 2 patients with MI post-percutaneous coronary intervention. In conclusion, this study sheds light on the potential utility of $\text{Na}[^{18}\text{F}]\text{F}$ PET/CT as a hot-spot imaging modality for myocardial IRI.

Keywords

$\text{Na}[^{18}\text{F}]\text{F}$, positron emission tomography, computed tomography, myocardial infarction, ischemia–reperfusion injury

Introduction

Sodium [^{18}F]fluoride ($\text{Na}[^{18}\text{F}]\text{F}$) uptake on positron emission tomography (PET)/computed tomography (CT) has been shown to be useful for imaging of vascular calcification.¹ Ion exchange between the fluoride ions and the hydroxyl group of hydroxyapatite crystals has been believed to be the major mechanism for $\text{Na}[^{18}\text{F}]\text{F}$ uptake in the calcified atherosclerotic area.^{1,2} Macrocalcification of the coronary vasculature, which is usually visualized with CT, is the hallmark of long-term cardiovascular mortality,³ whereas microcalcification of a vulnerable coronary atherosclerotic plaque, which is assessed with $\text{Na}[^{18}\text{F}]\text{F}$ PET/CT, appears to be a risk factor for acute myocardial infarction (MI).⁴ The identification of vulnerable coronary plaques is one of the main research subjects in modern cardiology; therefore, $\text{Na}[^{18}\text{F}]\text{F}$ PET/CT is a promising noninvasive modality for screening patients at high risk of fatal cardiovascular diseases.^{5,6}

In a previous study, $\text{Na}[^{18}\text{F}]\text{F}$ uptake was demonstrated in MI.⁷ In this previous study, myocardial apoptosis was found to be closely associated with $\text{Na}[^{18}\text{F}]\text{F}$ uptake in a rat model of

permanent coronary ligation, whereas calcium was not related to $\text{Na}[^{18}\text{F}]\text{F}$ uptake. Therefore, the uptake mechanism of $\text{Na}[^{18}\text{F}]\text{F}$ might be more complex in MI than in atherosclerotic diseases, and these mechanisms need to be elucidated in

¹ Department of Nuclear Medicine, Seoul National University Bundang Hospital, Seoul National University College of Medicine, Seoul, Korea

² Department of Internal Medicine, Seoul National University Bundang Hospital, Seoul National University College of Medicine, Seoul, Korea

³ Department of Radiology, Seoul National University Bundang Hospital, Seoul National University College of Medicine, Seoul, Korea

⁴ Institute of Radiation Medicine, Medical Research Center, Seoul National University, Seoul, Korea

Submitted: 25/10/2016. Revised: 10/01/2017. Accepted: 21/03/2017.

Corresponding Author:

Won Woo Lee, Department of Nuclear Medicine, Seoul National University Bundang Hospital, Seoul National University College of Medicine, 82, Gumi-ro 173 Beon-gil, Bundang-gu, Seongnam-si, Gyeonggi-do 13620, Seoul, Korea.
Email: wwlee@snu.ac.kr



order to widely use Na^{[18F]F} PET/CT for human cardiovascular diseases.

The present study aimed to investigate whether Na^{[18F]F} PET/CT can be used for imaging of ischemia–reperfusion injury (IRI) in a rat IRI model and in human MI cases after primary percutaneous coronary intervention (PCI). The traditional rat MI model was also employed as a reference to the rat IRI model. However, in the present study, we mainly focused on IRI because a rat MI model generated through permanent coronary ligation may not adequately reflect the clinical situations of most human MI cases that accompany some degree of reperfusion injury from thrombolysis or primary PCI.⁸

Materials and Methods

Rats

Eight-week-old male Sprague-Dawley rats (350 ± 10 g) were used throughout the study. For the IRI experiment, 28 rats were used for PET/CT imaging and subsequent histology (n = 10), autoradiography and histology (n = 5), area-at-risk assessment (n = 5), and CysA/saline effects evaluation (n = 8), respectively. For the MI experiment, 8 rats underwent the surgery and were evaluated for dynamic PET/CT imaging (n = 3) and histology (n = 5). The rats were cared for in a temperature- and humidity-controlled animal dedicated facility, which was accredited by the Association for Assessment and Accreditation of Laboratory Animal Care International. The animal experiment protocol was reviewed and approved by the institutional animal welfare committee.

Rat IRI

For the IRI surgery, after anesthesia induction with 0.3 mL of a 3:2 (vol/vol) mixture of tiletamine–zolazepam intraperitoneally, rats were intubated and maintained under ventilation (model 683, Harvard Apparatus, South Natick, Massachusetts) with oxygen supply at 2 to 5 L/min. The left anterior descending coronary artery was ligated for 35 minutes at the level of auricular appendage using a 4-0 silk suture and then released for 24 hours till the PET/CT study. Five minutes prior to the ligation removal, cyclosporine A (CysA; Sandimmun INJ, Novartis) at a dose of 10 mg/kg was injected through the tail vein to see whether the treatment effect can be monitored using the Na^{[18F]F} PET/CT. Ischemia–reperfusion injury rats for control had normal saline injection at the same volume with CysA injection (Supplemental Figure S1).

Rat MI

The MI rat model was generated via permanent ligation of the left anterior descending coronary artery. The MI rats were used for the determination of the optimal imaging time for Na^{[18F]F} PET/CT (Supplemental Figure S2) and histological comparison with IRI. Other experimental conditions for MI were the same with those for IRI.

Sodium [¹⁸F]fluoride PET/CT in Rats

Sodium [¹⁸F]fluoride PET/CT was performed 24 hours after IRI using an animal-dedicated PET/CT scanner (NanoPET/CT, Mediso, Budapest, Hungary). During PET/CT imaging, the temperature was maintained at 37°C, and inhalation anesthesia (2%–3% of isoflurane in 2–5 L/min of oxygen) was applied to the rats using a specialized animal-holding station (Minerva system, Mediso). Sodium [¹⁸F]fluoride was produced using an in-house 13-MeV cyclotron (Kotron13, Samyoung Unitech, Yongin-si, Gyeonggi-do, South Korea), and the injected dose was 11.1 to 18.5 MBq. The PET parameters were as follows: field of view per bed, 94.7 mm; acquisition coincidence mode, 1 to 5; energy window, 400 to 600 keV; and coincidence window, 5 ns. The PET images were reconstructed using the following parameters: reconstruction algorithm, 3-dimensional expectation-maximization; image matrix, 110 × 110 × 234; and voxel size, 0.4 × 0.4 × 0.4 mm. The spatial resolution of the PET images was 1.2 mm. Computed tomography images were obtained using the following parameters: projection number, 240; pitch, 1; tube voltage, 55 kVp; tube current, 145 μA; exposure, 28.0 mA; and exposure time, 1100 ms. Iodinated contrast agent (Ultravist370, Bayer, Leverkusen, Germany) was infused during the CT image acquisition (3 mL/10 min). Computed tomography images were reconstructed using the following parameters: filter, Butterworth; matrix, 332 × 332 × 473; and voxel size, 0.2116 × 0.2116 × 0.2116 mm. The CT resolution was 48 μm. The reconstructed PET/CT images were analyzed using quantitative software (PMOD version 3.508, PMOD Technologies, Zurich, Switzerland). Sodium [¹⁸F]fluoride uptake was quantitated with the standardized uptake value (SUV) over the infarct area, which was calculated as follows:

$$\text{SUV} = \frac{(\text{decay} - \text{corrected activity in kBq/cc}) \times (\text{weight in gram})}{\text{injected activity in kBq}}$$

Polar map images were produced using image analysis software (Carimas 2.8; Turku PET Centre, Turku, Finland), and a 17-myocardial segment model was employed.

2,3,5-Triphenyl-2H-Tetrazolium Chloride Staining

After PET/CT image acquisition, the rats were euthanized, and the abdomen was opened. Normal saline (30 mL) was then infused through the inferior vena cava to flush out blood, 2% solution of 2,3,5-triphenyl-2H-tetrazolium chloride (TTC) was infused (30 mL) through the ascending aorta into the left ventricle, and the hearts were harvested. The hearts were incubated for 1 hour at 37°C in 4% paraformaldehyde (PFA), with light protection. The hearts were then sectioned into 1-mm-thick slices using a slicer (Zivic Instruments, Pittsburgh, Pennsylvania), and the myocardial slices were scanned using a flat-bed scanner (G4010; Hewlett-Packard, Palo Alto, California). The percentage infarct size (100 × TTC-negative area/whole myocardial area) was measured with planimetry over the distal 3 myocardial rings, excluding the first apical myocardial ring. Image analysis software (Image J, 1.45S, NIH, Bethesda, Maryland) was used for the planimetric analysis.

Terminal Deoxynucleotidyl Transferase dUTP Nick End Labeling Assay

Myocardial apoptosis was evaluated with the terminal deoxynucleotidyl transferase dUTP nick end labeling (TUNEL) assay using a commercialized kit (In Situ Cell Death Detection kit, POD, Roche Diagnostics Co, Mannheim, Germany). The TTC-stained myocardial slices were cut into 4- μ m-thick sections. After deparaffinization, washing in a graded series of ethanol, and rehydration, the sections were fixed in 4% PFA in phosphate-buffered saline (PBS) for 15 minutes. After incubation with proteinase K solution at room temperature, equilibrium buffer was applied to the sections. The terminal deoxynucleotidyl transferase (TdT) reaction mix was then applied for 60 minutes at 37°C in a humidified chamber. The reaction was stopped by applying $\times 2$ saline-sodium citrate buffer for 15 minutes. The sections were washed in PBS, 0.3% hydrogen peroxide for 5 minutes, and then PBS. Streptavidin-horseradish peroxidase conjugate (Roche Diagnostics Co) was applied at room temperature for 30 minutes, and then, 3,3'-diaminobenzidine (Roche Diagnostics Co) staining was performed. The sections were immersed in deionized water and then mounted.

Calcium Staining

Von Kossa staining was performed over the 4- μ m-thick myocardial slices. A 5% silver nitrate solution was applied, and the slices were exposed to a 60-W lamp for 1 hour. After washing the slices thrice with distilled water, 5% hypo was applied. The slices were then washed again and were mounted.

Histone-1 Expression

The histone-1 targeting peptide (ApoPep-1) has been shown to be useful for evaluating apoptosis.⁹ It was conjugated with a red fluorescent dye (AHR-553, BioActs, Incheon, South Korea), and the dye-conjugated peptide (excitation and emission wavelengths of 561 nm and 589 nm, respectively) was intravenously injected (100 nmol) 2 hours before the rats were killed. One-mm-thick myocardial rings were imaged using a fluorescence imaging system (Lumina II, Perkin-Elmer, Waltham, Massachusetts) at 535 nm excitation and 583 nm emission.

Autoradiography

The 1-mm-thick myocardial rings from the TTC-stained heart that was harvested after Na^{[18F]F} injection (dose, 11.1-18.5 MBq) were exposed to phosphor imaging plates for 20 to 24 hours, and the exposed plates were scanned using a laser scanning system (Typhoon FLA 7000, GE Healthcare, Waukesha, Wisconsin). The scanning condition was photomultiplier tube = 1000, pixel size = 25 μ m, and L4.

Evaluation of the Area-at-Risk for Na^{[18F]F} Uptake

Rats underwent the IRI procedure involving ischemic injury for 35 minutes (Supplemental Figure S1). At 35 minutes from

Table 1. Patient Characteristics.

	IRI Patients With MI Post-PCI		Control
Age	52	57	67
Sex	Male	Male	Male
MI type	STEMI (VI-V5)	Non-STEMI	NA
CK-MB, ng/mL ^a	266.4	123.8	NA
Troponin I, ng/mL ^b	189	11.3	NA
Culprit vessel	LAD artery, proximal	RCA, mid	NA
Chest pain onset to PCI	4 hours	3 hours	NA
PCI to PET/CT	47 hours	11 hours	NA
Comorbidity	Diabetes for 10 years	Heavy smoker (2 packs for 30 years)	Renal cancer
Medication prior to MI	Sarpogrelate 100 mg twice daily, glimepiride 2 mg twice daily, metformin 500 mg twice daily	None	None
Abciximab during PCI	None	Yes, after thrombus suction	NA

Abbreviations: CK, creatine kinase; IRI, ischemia-reperfusion injury; LAD, left anterior descending; MI, myocardial infarction; NA, not applicable; PCI, primary percutaneous coronary intervention; PET/CT, positron emission tomography/computed tomography; RCA, right coronary artery; STEMI, ST-segment elevation myocardial infarction.

^aNormal range of CK-MB = 0 to 2.8 ng/mL.

^bnormal range of troponin I = 0 to 0.045 ng/mL.

coronary ligation, the coronary ligature was loosened enough for reperfusion but was not completely removed in order to evaluate the area-at-risk from IRI. After 24 hours, Na^{[18F]F} was intravenously injected (dose, 11.1-18.5 MBq), and the thoracic cage was reopened. The coronary ligature was tightened to achieve reocclusion of coronary flow. Then, a retrograde injection of 2 mL of Evans-blue dye (3% [wt/vol] mixture of PBS, Sigma-Aldrich, St Louis, Missouri) was delivered into the left ventricle through the ascending aorta. The heart was immediately harvested and stored at -20°C for 1 hour. Using a slicer (Zivic Instruments), the frozen heart was sliced into 1-mm-thick myocardial rings. The myocardial slices were immersed in freshly prepared 2% TTC solution at 37°C for 20 minutes. After fixation with 4% PFA for 80 minutes, the slices were scanned using a flat-bed scanner (G4010, Hewlett-Packard) and were placed on a phosphor imaging plate for 20 to 24 hours. A laser scanner (Typhoon FLA 7000, GE Healthcare) was used to identify the Na^{[18F]F} signal at the area at risk.

Patients With IRI

The study included 2 patients with MI (Table 1). The 2 patients were confirmed with MI based on clinical, biochemical, and angiographic (total occlusion by thrombus) results. Primary PCI was performed in the patients, and drug-eluting stents were successfully inserted at the culprit vessels after thrombus

aspiration. One patient was administered a glycoprotein IIb/IIIa inhibitor (Abciximab, ReoPro, Eli Lilly, Indianapolis, Indiana) during PCI (0.25 mg/kg IV bolus administration immediately after thrombus suction prior to balloon dilatation, and then 0.125 µg/kg/min IV continuous infusion for 12 hours) to prevent reperfusion injury, while the other patient did not receive abciximab injection at the discretion of the attending cardiologist. After PCI, the 2 patients did not complain of chest pain. Other cardioprotective medications, such as aspirin, clopidogrel, atorvastatin, perindopril, and carvedilol, were administered after the PCI procedure. Two-dimensional echocardiography revealed wall motion abnormality in the corresponding MI area. In addition, another patient was used as a control. This control patient underwent Na^[18F]F PET/CT for the evaluation of possible bone metastasis of renal cancer (Table 1). The patients provided informed consent, and the human study was approved by the institutional review board (B-1312/232-303).

Sodium [¹⁸F]fluoride PET/CT Studies in Humans

A PET scanner integrated with a 64-channel multidetector CT system (GE Healthcare) was used in the human studies. The injected dose of Na^[18F]F was 5.18 MBq (0.14 mCi) per kg body weight. Computed tomography images were acquired just before PET acquisition. The CT parameters were as follows: tube potential, 120 kVp; tube current, 60 to 210 mA; beam collimation, 40 mm (0.625 × 64); pitch factor, 0.516:1; coverage speed, 41.24 mm/s; and tube rotation time, 0.5 s. Iodine contrast agent was not used in the CT studies. The CT radiation exposure was 5.13 to 32.03 mGy using CTDI_{vol} and 227.13 to 614.07 mGy cm using dose length product. Positron emission tomography images (axial field of view per bed, 15.4 cm; acquisition time per bed, 5 minutes) covering the lower chest were obtained 60 minutes after injection of Na^[18F]F. The PET images were scatter- and attenuation corrected with an iterative reconstruction algorithm (OSEM, 20 subsets and 2 iterations). The reconstructed PET images were analyzed in the Carimas software (version 2.8; Turku PET Centre) to produce a polar map.

Statistical Analysis

Nonparametric analysis was performed to compare the SUV and the MI size between the CysA and control rat groups. Statistical software (MedCalc version 12.4.0.0; MedCalc, Mariakerke, Belgium) was employed. A *P* value of <.05 was considered significant.

Results

Sodium [¹⁸F]fluoride PET/CT Findings in Rat IRI

Positron emission tomography images were obtained for 30 minutes from 60 minutes post-injection. This time was determined through dynamic Na^[18F]F PET/CT studies that showed the uptake plateau at 60 minutes post-injection of

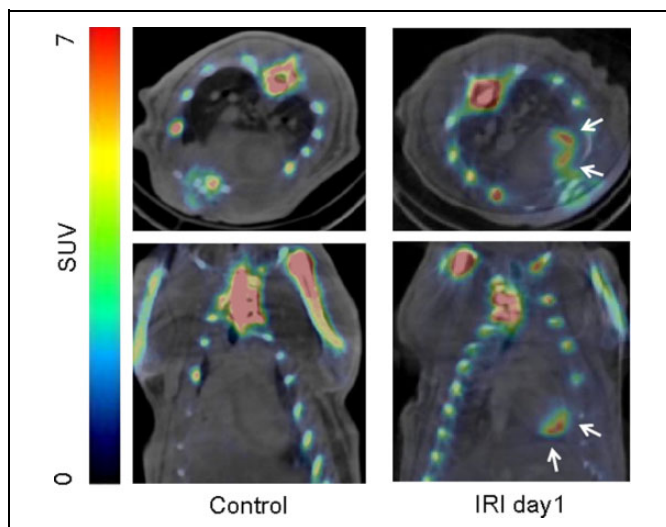


Figure 1. Sodium [¹⁸F]fluoride (Na^[18F]F) positron emission tomography (PET)/computed tomography (CT) in vivo in a rat 24 hours after ischemia–reperfusion injury (IRI). A rat with sham operation was used as a control. The rat with IRI showed prominent uptake of Na^[18F]F in the myocardium of the left ventricle (white arrows).

Na^[18F]F in MI with permanent coronary ligation (*n* = 3; Supplemental Figure S2). Using the optimized protocol, the prominent uptake of Na^[18F]F was readily observed in the myocardium of left ventricle 24 hours post-IRI in all the rats investigated (*n* = 10; Figure 1) and the subsequent ex vivo PET/CT imaging of myocardial slices revealed that Na^[18F]F uptake was present in TTC-negative and TUNEL-positive areas (Figure 2A). Furthermore, autoradiography showed that the infarct sites were positive for Na^[18F]F uptake, negative for TTC staining, and positive for histone-1 expression (*n* = 5 rats; Figure 2B). However, the area-at-risk that showed negative Evans-blue staining (due to blood flow impairment) and positive TTC staining (noninfarct) was negative for Na^[18F]F uptake in other 5 rats that tested (Figure 2C). Calcification was found in the TTC-negative area of the IRI rats (reperfused MI); however, the TTC-negative area of MI rats with permanent coronary ligation was negative for calcium staining (nonreperfused MI) in all the rats that were ever tested (Figure 2D).⁷ Myocardial apoptosis, which was identified with positive histone-1 expression and TUNEL staining, was often found in the area at risk adjacent to a TTC-negative infarct in the IRI model but not in the MI model (arrows in Figure 2D).

Monitoring of Therapeutic Efficacy Using Na^[18F]F PET/CT

Cyclosporine A was intravenously injected through the tail vein 5 minutes prior to ligation removal in order to ameliorate the reperfusion injury (Supplemental Figure S1; *n* = 4 rats).¹⁰ Normal saline was used as a control (*n* = 4 rats). Sodium [¹⁸F]fluoride uptake in the IRI area appeared prominent and distinct in the saline group, and substantially reduced in the CysA group (Figure 3). The quantitation of Na^[18F]F uptake in

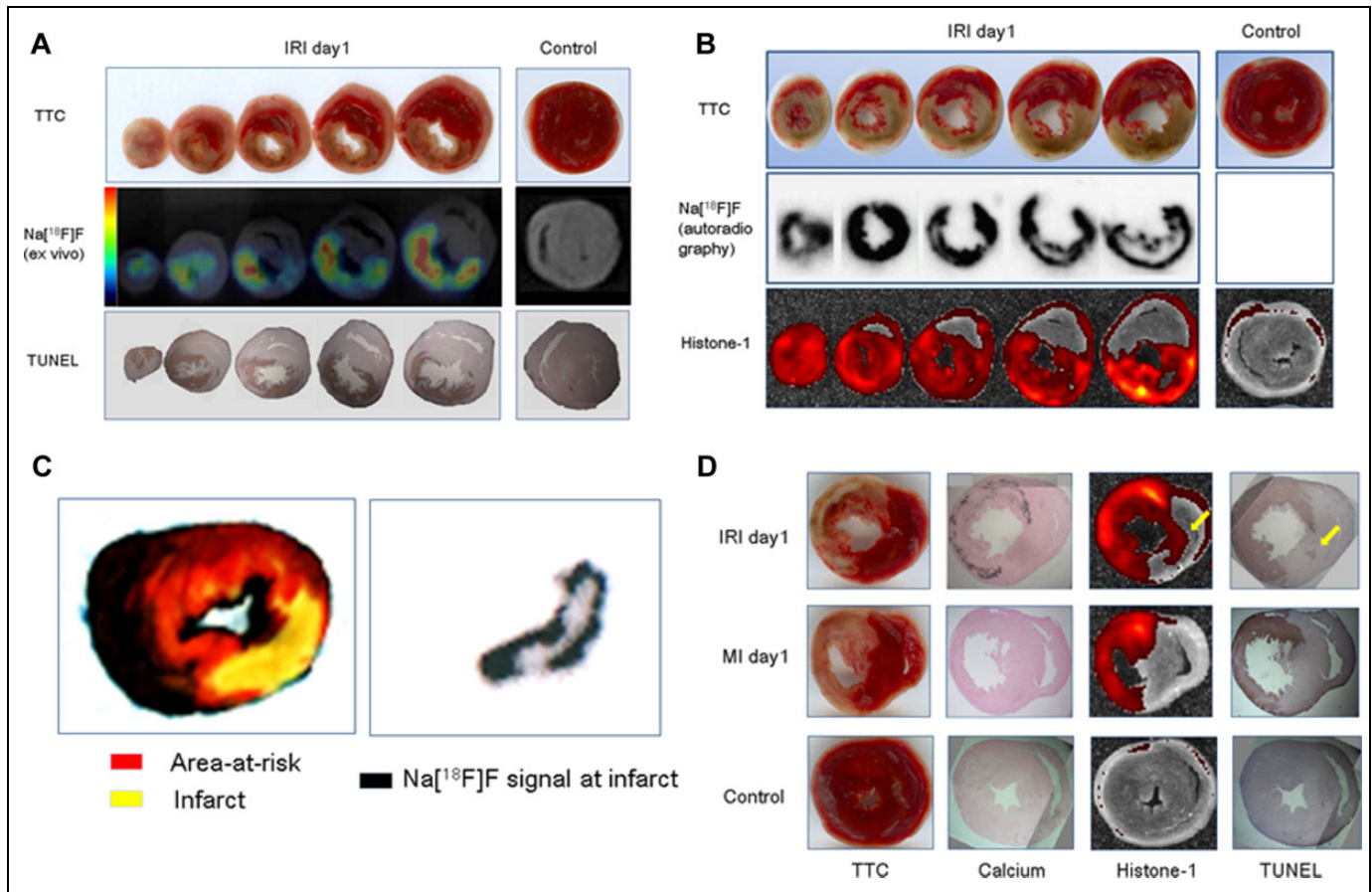


Figure 2. Sodium [^{18}F]fluoride ($\text{Na}[^{18}\text{F}]\text{F}$) uptake ex vivo. (A) Immediately after the in vivo positron emission tomography (PET)/computed tomography (CT) acquisition, the rats were killed, and the hearts were harvested and 2,3,5-triphenyl-2H-tetrazolium chloride (TTC)-stained. The hearts were sliced into 1-mm-thick myocardial rings. Then ex vivo PET/CT was acquired for 1 hour. The myocardial rings were sectioned into 4- μm -thick slices and then stained for apoptosis (terminal deoxynucleotidyl transferase dUTP nick end labeling [TUNEL] staining). (B) $\text{Na}[^{18}\text{F}]\text{F}$ autoradiography of the myocardial rings. The TTC-negative area was matched with $\text{Na}[^{18}\text{F}]\text{F}$ -positive and myocardial apoptosis area. Myocardial apoptosis was evaluated using a peptide targeting histone-1. (C) Area at risk was negative for $\text{Na}[^{18}\text{F}]\text{F}$ uptake. The area at risk was Evans-blue staining negative but TTC staining positive (left panel). The infarct area with negative TTC staining was positive for $\text{Na}[^{18}\text{F}]\text{F}$ signal, but the area at risk was negative for $\text{Na}[^{18}\text{F}]\text{F}$ uptake in the autoradiography study (right panel). (D) Comparisons of ischemia-reperfusion injury (IRI) versus myocardial infarction (MI) regarding calcium staining, histone-1 expression, and TUNEL staining. The calcium accumulation was prominent in the IRI model but absent in the MI model. Myocardial apoptosis was often observed in the noninfarcted myocardial area adjacent to TTC negative infarct in the IRI model (arrows) but not in the MI model.

the infarct showed that the SUV was significantly lower in the CysA group than in the saline group (1.20 ± 0.70 vs 2.16 ± 0.22 ; $P = .0286$ by the Mann-Whitney U test). Infarct size was also significantly lower in the CysA group than in the saline group ($36.16\% \pm 11.18\%$ vs $54.17\% \pm 13.50\%$; $P = .0041$ by the Mann-Whitney U test; Figure 3). The remote myocardium was also assessed for SUV change after CysA administration (Supplemental Figure S3). No SUV change was observed in the remote myocardium before and after CysA administration (0.34 ± 0.07 vs 0.34 ± 0.09 ; $P = .7728$ by the Mann-Whitney U test).

Sodium [^{18}F]fluoride PET/CT Findings in Human IRI

The study included 2 male patients who had undergone PCI for acute MI before $\text{Na}[^{18}\text{F}]\text{F}$ PET/CT (Table 1). The first patient

was a 52-year-old man with ST-segment elevation MI (STEMI). Thrombosuction and drug-eluting stent insertion effectively reduced his chest pain. The time from chest pain onset to reperfusion therapy was estimated to be 4 hours. One day later, echocardiography revealed severe hypokinesia in the apico-mid antero-septal wall and apico-mid anterior wall. Sodium [^{18}F]fluoride PET/CT was performed on day 2 after PCI (47 hours after reperfusion therapy). Increased uptake of $\text{Na}[^{18}\text{F}]\text{F}$ was noted in the anterior and anteroseptal walls (Figure 4A and B). Additionally, the polar map clearly demonstrated increased $\text{Na}[^{18}\text{F}]\text{F}$ uptake in the left anterior descending coronary artery territory with an SUVmax of 1.6 (Figure 4C). The second patient was a 57-year-old man with non-STEMI. In this patient, immediately after the thrombus suction procedure, abciximab was injected (0.25 mg/kg IV bolus administration, and then 0.125 microgram/kg/min IV

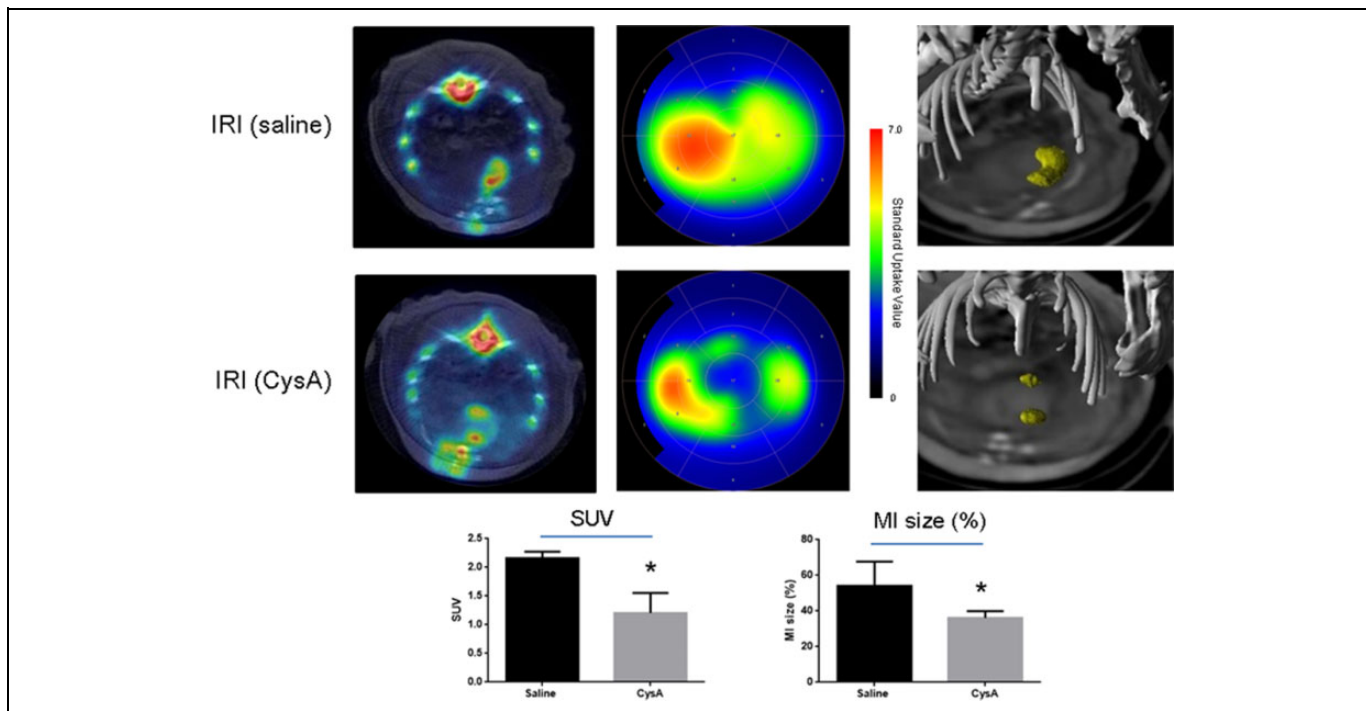


Figure 3. The effect of cyclosporine A (CysA) on ischemia–reperfusion injury ($n = 4$) as demonstrated with sodium [^{18}F]fluoride ($\text{Na}[^{18}\text{F}]\text{F}$) positron emission tomography (PET)/computed tomography (CT) compared to control ($n = 4$). The standardized uptake value (SUV) was significantly lower in the CysA group than in the saline group (1.20 ± 0.70 vs 2.16 ± 0.22 ; $P = .0286$). Furthermore, the percentage infarct size was significantly lower in the CysA group than in the saline group ($36.16\% \pm 11.18\%$ vs $54.17\% \pm 13.50\%$; $P = .0041$).

continuous infusion for 12 hours) to reduce reperfusion injury from distal embolism during thrombosuction. Balloon dilatation was then performed. His chest pain subsided soon after PCI, and the time from chest pain onset to reperfusion therapy was 3 hours. On the next day, echocardiography revealed hypokinesia in the mid-basal inferior wall. Sodium [^{18}F]fluoride PET/CT was performed on the same day of PCI (11 hours after reperfusion therapy). Increased uptake of $\text{Na}[^{18}\text{F}]\text{F}$ was noticed in the basal inferior wall (Figure 4D and E). A polar map also showed $\text{Na}[^{18}\text{F}]\text{F}$ uptake in the corresponding basal right coronary artery territory with an SUVmax of 1.1 (Figure 4F). In a control patient (Table 1), no discernible $\text{Na}[^{18}\text{F}]\text{F}$ uptake was observed in the myocardium (Figure 4G-I).

Discussion

In the present study, $\text{Na}[^{18}\text{F}]\text{F}$ uptake on myocardial IRI was readily demonstrated in both rats and humans using PET/CT. The myocardial infarct, identified as a TTC-negative area, always showed corresponding $\text{Na}[^{18}\text{F}]\text{F}$ uptake, whereas the area at risk was negative for $\text{Na}[^{18}\text{F}]\text{F}$ uptake. Therefore, $\text{Na}[^{18}\text{F}]\text{F}$ PET/CT played a role as a hot-spot imaging modality for myocardial IRI, with in vivo $\text{Na}[^{18}\text{F}]\text{F}$ uptake being a surrogate of ex vivo TTC staining. In addition, myocardial apoptosis and calcification were also found to be associated with $\text{Na}[^{18}\text{F}]\text{F}$ uptake in the IRI myocardium.

It was interesting to find the differences in the underlying histopathology between reperfused infarct from the IRI model

and nonreperfused infarct from the MI model (permanent coronary ligation), because calcium accumulation was never observed in MI but appeared prominent in IRI using the same rat model (Figure 2D).⁷ The amount of accumulated calcium might be greater in the IRI, above the detection threshold for Von Kossa staining method, than in the MI, below the threshold. Reperfusion might have increased the delivery of calcium particularly to the infarct border zone, which was readily appreciated by the peripheral uptake pattern of calcium staining and $\text{Na}[^{18}\text{F}]\text{F}$ autoradiography (Figures 2B-D). These findings are reminiscent of “doughnut sign” of $^{99\text{m}}\text{Tc}$ -phosphate scintigraphy with central photon defect in MI.¹¹ Therefore, the myocardial injury by the IRI (ischemic plus reperfusion injury) may be different from that by the MI (ischemic injury alone). Furthermore, the noninfarcted myocardium adjacent to the TTC-negative infarct area sometimes showed evidence of myocardial apoptosis in the IRI model, which was not observed in the MI model (Figure 2D).

When it comes to the clinical application of $\text{Na}[^{18}\text{F}]\text{F}$ PET/CT, the history of $^{99\text{m}}\text{Tc}$ -phosphates is worthy of commenting. There have been many reports about the hot spot imaging of infarcted tissue using a variety of $^{99\text{m}}\text{Tc}$ -phosphates, but the peak uptake of $^{99\text{m}}\text{Tc}$ -phosphates was often delayed as late as 12 to 24 hours post-infarction.^{12,13} Moreover, the $^{99\text{m}}\text{Tc}$ -phosphates uptake would not last long enough for the infarct size to be stably measured.^{12,14} We believe that one possible clinical application of $\text{Na}[^{18}\text{F}]\text{F}$ PET/CT lies in the monitoring of the preventive effects for reperfusion injury,

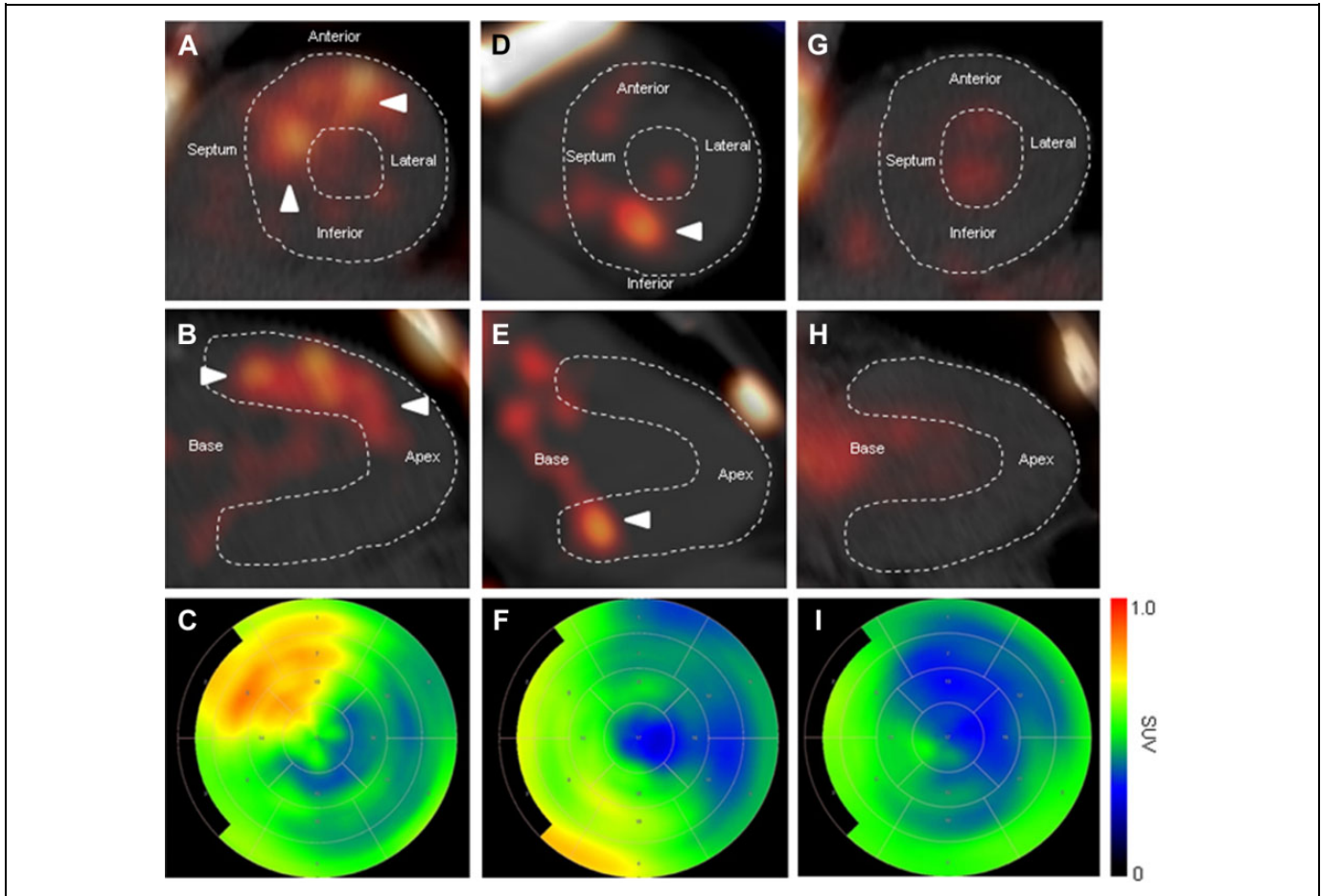


Figure 4. Sodium [^{18}F]fluoride ($\text{Na}[^{18}\text{F}]\text{F}$) positron emission tomography (PET)/computed tomography (CT) in humans with ischemia-reperfusion injury (IRI). (A-C) $\text{Na}[^{18}\text{F}]\text{F}$ PET/CT findings without antireperfusion injury therapy. A 52-year-old man with ST-segment elevation myocardial infarction (STEMI) in the left anterior descending (LAD) artery territory underwent percutaneous coronary intervention (PCI) in the LAD artery, and $\text{Na}[^{18}\text{F}]\text{F}$ PET/CT was performed 47 hours after PCI. Short-axis (A) and vertical long-axis images (B) showed an increase in $\text{Na}[^{18}\text{F}]\text{F}$ uptake in the anterior and septal walls (arrows). (C) A polar map image showed an increase in $\text{Na}[^{18}\text{F}]\text{F}$ uptake in the apico-mid anterior and apico-mid anteroseptal walls. The SUVmax was 1.6. (D-F) $\text{Na}[^{18}\text{F}]\text{F}$ PET/CT findings with antireperfusion injury therapy. A 57-year-old man with non-STEMI in the right coronary artery (RCA) territory underwent PCI in the RCA and $\text{Na}[^{18}\text{F}]\text{F}$ PET/CT on the same day with an interval of 11 hours. Short-axis (D), vertical long-axis (E) (arrows), and polar map (F) images showed an increase in $\text{Na}[^{18}\text{F}]\text{F}$ uptake in the basal inferior wall. The SUVmax was 1.1. The extent and intensity of $\text{Na}[^{18}\text{F}]\text{F}$ uptake were less severe in this patient (D-F) than those in the LAD patient with STEMI without anti-reperfusion injury therapy (A-C). (G-I) $\text{Na}[^{18}\text{F}]\text{F}$ PET/CT in a 67-year-old man with renal cancer (control). (G) Short-axis image. (H) Vertical long-axis image. (I) Polar map image.

thereby discriminating ischemic injury from reperfusion injury (Figure 3).^{15,16} Positron emission tomography/CT readily showed a decrease in $\text{Na}[^{18}\text{F}]\text{F}$ uptake in the myocardium after CysA administration in conjunction with a reduction in the infarct size. The preventive efficacy of CysA for reperfusion injury was identified using PET/CT, along with the SUV, which is a clinically proven quantitative parameter. The difference in $\text{Na}[^{18}\text{F}]\text{F}$ uptake before and after CysA treatment may represent the amount of myocardium at risk of reperfusion injury (rescued by CysA), whereas the remaining $\text{Na}[^{18}\text{F}]\text{F}$ uptake after CysA administration may reflect the magnitude of genuine ischemic injury free from reperfusion injury (assuming complete prevention of reperfusion injury by CysA).^{10,17} If $\text{Na}[^{18}\text{F}]\text{F}$ PET/CT were routinely performed after CysA treatment, the $\text{Na}[^{18}\text{F}]\text{F}$ uptake might be useful for

prognosis prediction, as a final integrated result of the original ischemic injury and the unprotected reperfusion injury post-CysA. Among our 2 patients who had MI, 1 patient underwent antiplatelet treatment for amelioration of reperfusion injury, and the extent and intensity of $\text{Na}[^{18}\text{F}]\text{F}$ uptake were lower in this patient than in the other patient who did not receive antiplatelet treatment (Figure 4). Of course, it is too early to confirm the utility of $\text{Na}[^{18}\text{F}]\text{F}$ PET/CT as an imaging biomarker for human IRI. Nonetheless, a hot-spot imaging modality with quantitative capability would be a useful monitoring tool for the management of IRI.

It is important to note the recent failure of CysA preventive trials for human IRI.^{17,18} Therefore, rat IRI results may not directly extrapolate to human IRI. However, previous experimental studies strongly suggest the usefulness of CysA for

IRI.¹⁹⁻²⁴ Sodium [¹⁸F]fluoride PET/CT may facilitate the development of anti-IRI therapy by objectively demonstrating the PCI effect, unveiling the final integrated result of the original ischemic injury and the reperfusion injury post-PCI. Furthermore, the pattern and location of Na[¹⁸F]F uptake may provide the cardiologist with valuable information regarding the PCI effect as seen in our results (Figure 3), which is not possible by only measuring the blood markers of myocardial injury. Further studies are warranted in this regard.

Sodium [¹⁸F]fluoride has been shown to be a safe and effective radiopharmaceutical for the detection of bone metastasis in humans,¹⁹⁻²² and PET/CT has been shown to be a robust imaging tool, especially for the quantification of imaging biomarkers.²³⁻²⁵ The combination of the 2 would pave the way for noninvasive imaging of myocardial injury, and the present study demonstrates the potential usefulness of Na[¹⁸F]F PET/CT in the management of IRI.

Conclusion

Ischemia–reperfusion injury was readily visualized in rats and humans using Na[¹⁸F]F PET/CT. Sodium [¹⁸F]fluoride uptake in the IRI was matched with the TTC-negative infarct. The preventive effect of anti-IRI treatment was noninvasively assessed using the Na[¹⁸F]F PET/CT. Sodium [¹⁸F]fluoride PET/CT is a promising hot-spot imaging modality for IRI.

Authors' Note

WWL and YSC designed the studies. JHH and SYL performed the animal experiments. HC and WWL analyzed the data and wrote the manuscript. EJC performed the human PET/CT studies. All the patients provided their informed consents. Compliance With Ethical Standards: Research involving Human Participants: The study was approved by an institutional review board and has been performed in accordance with the ethical standards laid down in the 1964 Declaration of Helsinki and its later amendments.

Declaration of Conflicting Interests

The author(s) declared no potential conflicts of interest with respect to the research, authorship, and/or publication of this article.

Funding

The author(s) disclosed receipt of the following financial support for the research, authorship, and/or publication of this article: This study was supported in part by the Basic Science Research Program through the National Research Foundation of Korea funded by the Ministry of Education (2015R1D1A1A01059146) and by Seoul National University Bundang Hospital Research Fund (14-2016-012).

Supplemental Material

The online supplemental figures are available at <http://journals.sagepub.com/doi/suppl/10.1177/1536012117704767>.

References

- Irkle A, Vesey AT, Lewis DY, et al. Identifying active vascular microcalcification by (18)F-sodium fluoride positron emission tomography. *Nat Commun*. 2015;6:7495.
- Blau M, Ganatra R, Bender MA. 18 F-fluoride for bone imaging. *Semin Nucl Med*. 1972;2(1):31–37.
- Budoff MJ, Shaw LJ, Liu ST, et al. Long-term prognosis associated with coronary calcification: observations from a registry of 25,253 patients. *J Am Coll Cardiol*. 2007;49(18):1860–1870.
- Joshi NV, Vesey AT, Williams MC, et al. 18F-fluoride positron emission tomography for identification of ruptured and high-risk coronary atherosclerotic plaques: a prospective clinical trial. *Lancet*. 2014;383(9918):705–713.
- Derlin T, Richter U, Bannas P, et al. Feasibility of 18F-sodium fluoride PET/CT for imaging of atherosclerotic plaque. *J Nucl Med*. 2010;51(6):862–865.
- Chen W, Dilsizian V. Targeted PET/CT imaging of vulnerable atherosclerotic plaques: microcalcification with sodium fluoride and inflammation with fluorodeoxyglucose. *Curr Cardiol Rep*. 2013;15(6):364.
- Han JH, Lim SY, Lee MS, Lee WW. Sodium [(18)F]fluoride PET/CT in myocardial infarction. *Mol Imaging Biol*. 2015;17(2):214–221.
- Gibbons RJ, Valeti US, Araoz PA, Jaffe AS. The quantification of infarct size. *J Am Coll Cardiol*. 2004;44(8):1533–1542.
- Wang K, Purushotham S, Lee JY, et al. In vivo imaging of tumor apoptosis using histone H1-targeting peptide. *J Control Release*. 2010;148(3):283–291.
- Piot C, Croisille P, Staat P, et al. Effect of cyclosporine on reperfusion injury in acute myocardial infarction. *N Engl J Med*. 2008;359(5):473–481.
- Rude RE, Parkey RW, Bonte FJ, et al. Clinical implications of the technetium-99m stannous pyrophosphate myocardial scintigraphic “doughnut” pattern in patients with acute myocardial infarcts. *Circulation*. 1979;59(4):721–730.
- Bonte FJ, Parkey RW, Graham KD, Moore J, Stokely EM. A new method for radionuclide imaging of myocardial infarcts. *Radiology*. 1974;110(2):473–474.
- Siegel BA, Engel WK, Derrer EC. Localization of technetium-99m diphosphonate in acutely injured muscle. Relationship to muscle calcium deposition. *Neurology*. 1977;27(3):230–238.
- Willerson JT, Parkey RW, Bonte FJ, Meyer SL, Atkins JM, Stokely EM. Technetium stannous pyrophosphate myocardial scintigrams in patients with chest pain of varying etiology. *Circulation*. 1975;51(6):1046–1052.
- Duchen MR, McGuinness O, Brown LA, Crompton M. On the involvement of a cyclosporin A sensitive mitochondrial pore in myocardial reperfusion injury. *Cardiovasc Res*. 1993;27(10):1790–1794.
- Griffiths EJ, Halestrap AP. Protection by cyclosporin A of ischemia/reperfusion-induced damage in isolated rat hearts. *J Mol Cell Cardiol*. 1993;25(12):1461–1469.
- Cung TT, Morel O, Cayla G, et al. Cyclosporine before PCI in patients with acute myocardial infarction. *N Engl J Med*. 2015;373(11):1021–1031.
- Ottani F, Latini R, Staszewsky L, et al; CYCLE Investigators. Cyclosporine A in reperfused myocardial infarction: the multicenter, controlled, open-label CYCLE trial. *J Am Coll Cardiol*. 2016;67(4):365–374.

19. Kang JY, Lee WW, So Y, Lee BC, Kim SE. Clinical usefulness of (18)F-fluoride bone PET. *Nucl Med Mol Imaging*. 2010;44(1):55–61.
20. Lee SJ, Lee WW, Kim SE. Bone positron emission tomography with or without CT is more accurate than bone scan for detection of bone metastasis. *Korean J Radiol*. 2013;14(3):510–519.
21. Yoon SH, Kim KS, Kang SY, et al. Usefulness of (18)F-fluoride PET/CT in breast cancer patients with osteosclerotic bone metastases. *Nucl Med Mol Imaging*. 2013;47(1):27–35.
22. Lee H, Lee WW, Park SY, Kim SE. F-18 sodium fluoride positron emission tomography/computed tomography for detection of thyroid cancer bone metastasis compared with bone scintigraphy. *Korean J Radiol*. 2016;17(2):281–288.
23. Jo I, Zeon SK, Kim SH, et al. Correlation of primary tumor FDG uptake with clinicopathologic prognostic factors in invasive ductal carcinoma of the breast. *Nucl Med Mol Imaging*. 2015;49(1):19–25.
24. Lee JH, Lee GY, Kim SJ, et al. Imaging findings and literature review of (18)F-FDG PET/CT in primary systemic AL amyloidosis. *Nucl Med Mol Imaging*. 2015;49(3):182–190.
25. Yoo MY, Paeng JC, Cheon GJ, et al. Prognostic value of metabolic tumor volume on (11)C-methionine PET in predicting progression-free survival in high-grade glioma. *Nucl Med Mol Imaging*. 2015;49(4):291–297.